EFDA–JET–CP(12)06/31

M.F.F. Nave, L.-G. Eriksson, C. Giroud, J. S. de Grassie, T. Hellsten,
T. Johnson, K, Kirov, Y. Lin, J. Mailoux, P. Mantica, M.-L. Mayoral,
F.I. Parra, J. Ongena, T. Tala, A.Salmi, J.H.F. Severo, P. de Vries
and JET EFDA contributors

Scalings of Spontaneous Rotation in the JET Tokamak

Scalings of Spontaneous Rotation in the JET Tokamak

M.F.F. Nave[1], L.-G. Eriksson[2], C. Giroud[3], J. S. de Grassie[4], T. Hellsten[5], T. Johnson[5], K, Kirov[3], Y. Lin[6], J. Mailoux[3], P. Mantica[11], M.-L. Mayoral[3], F.I. Parra[6], J. Ongena[7], T. Tala[8], A.Salmi[8], J.H.F. Severo[9], P. de Vries[10]
and JET EFDA contributors*

JET-EFDA, Culham Science Centre, OX14 3DB, Abingdon, UK

[1]*Associação EURATOM/IST, Instituto de Plasmas e Fusão Nuclear, Instituto Superior Técnico, Universidade Técnica de Lisboa, 1049-001, Lisbon, Portugal*
[2]*European Commission, Research Directorate General, B-1049 Brussels, Belgium*
[3]*EURATOM-CCFE Fusion Association, Culham Science Centre, OX14 3DB, Abingdon, OXON, UK*
[4]*General Atomics, P.O. Box 85608, San Diego, California, USA*
[5]*Association EURATOM - VR, Fusion Plasma Physics, EES, KTH, Stockholm, Sweden*
[6]*Plasma Science and Fusion Center, Massachusetts Inst. of Technology, Cambridge, MA 02139, USA*
[7]*ERM-KMS, Association EURATOM-Belgian State, Brussels, Belgium*
[8]*Association Euratom-Tekes, VTT, Finland*
[9]*Institute of Physics, University of Sao Paulo, SP, Brazil*
[10]*FOM Institute DIFFER, Association EURATOM-FOM, the Netherlands*
[11]*Instituto di Fisica del Plasma, CNR-EURATOM, Milano, Italy*
** See annex of F. Romanelli et al, "Overview of JET Results",*
(24th IAEA Fusion Energy Conference, San Diego, USA (2012)).

Preprint of Paper to be submitted for publication in Proceedings of the
24th IAEA Fusion Energy Conference (FEC2012), San Diego, USA
8th October 2012 - 13th October 2012

ABSTRACT
This paper summarises and highlights experimental results from recent JET studies on intrinsic rotation [1-4]. Levels of intrinsic rotation measured in JET H-modes are generally lower than expected from scaling laws for co-current rotating plasmas that predict that rotation increases with normalised beta [5]. Both co- and counter-current is observed and there aren't significant differences between rotation observed in L-mode and H-mode plasmas. Experimentally several factors have been found to influence intrinsic rotation, such as fast ion losses and toroidal field ripple, suggesting that different physics mechanisms are at play to drive intrinsic rotation and that these should be taken into consideration when extrapolating to future devices. It is also apparent from JET data that independent mechanisms may be driving rotation in the edge and the plasma core. Toroidal field ripple, in particular, was found to have a significant effect on the intrinsic rotation of plasmas without momentum input. JET results suggest that ITER intrinsic rotation may be substantially less than what was previously predicted by the multi-machine rotation scaling of ref. [5].

1. INTRODUCTION
Plasma rotation is one of the central topics for toroidal plasma confinement and it is considered to play a key role in tokamak plasma performance. The question of whether intrinsic rotation, that is rotation measured in the absence of momentum input, would on its own or as a supplement to Neutral Beam Injection (NBI) induced rotation be sufficient to fulfill the requirements for high confinement plasmas such as the suppression of turbulence and stabilization of MHD modes is an important issue. In JET, a database of rotation in plasmas with no NBI momentum has been built that includes plasmas with Ohmic heating, ion-cyclotron radio-frequency (ICRF) heating and, lower hybrid current-drive (LHCD).

In addition, the effect of toroidal field ripple on intrinsic rotation was studied in plasmas with Ohmic and ICRF heating with ripple amplitudes that ranged from JET's standard low level of 0.08% to 1.5% Here we summarize experimental results and show highlights from recent publications [1, 4].

Rotation measurements shown here are from Charge Exchange Recombination Spectroscopy (CXRS) of C6 using the blip method [7], where measurements are done using a diagnostic NBI blip (a low power, short duration pulse of NBI). CXRS provide measurements of toroidal angular frequencies and ion temperatures in 12 radial positions that cover from the plasma center (typically at R~3m) to close to the edge (R~3.8). The time resolution is 10 ms. Data shown in this paper is from the first 10-30 ms when momentum from NBI is negligible. (Edge measurements with a higher radial resolution are also available, however the time resolution, 100ms, is too poor for intrinsic rotation studies.)

2. INTRINSIC ROTATION EXPERIMENTS (With JET standard low ripple ($\delta_{TF} = 0.08\%$))
Toroidal rotation has been measured in plasmas with ICRF, LHCD and Ohmic heating. Several ICRF heating schemes were used, some to produce direct electron heating including mode conversion

experiments, others to produce ion dominant heating. ICRF rotation measurements exist for L-modes [7,8] and H-modes [1,7,9]. Ohmic and LHCD measurements were all in L-mode plasmas. Typical C6 toroidal angular frequencies, $\omega < 10$ krad/s (corresponding to velocities <30km/s) are low and quite similar in all heating scenarios. These are one order of magnitude smaller than in discharges with rotation driven by NBI. Both co-current and counter-current rotation is observed as summarized in the table below. At the standard low toroidal field ripple of 0.8%, the edge is in most cases rotating in the cocurrent direction. Edge counter-rotation was observed in a few ELMy H-mode cases. The plasma core can be either co- or counter-rotating.

2.1 ICRF HEATING

Most intrinsic rotation experiments in JET were done with ICRF heating, powers up to 10MW, in plasmas with two ion species, the main plasma ion and a minority ion with concentrations from 1% to 20%. Depending on the relative concentration of the species, the application of ICRF waves involved two heating scenarios: minority heating and mode conversion. Rotation measurements were done using six ICRF heating schemes, three providing dominant ion heating and three giving direct electron heating. For dominant ion heating the following was used: D (H), i. e. D plasmas with H minority, with 1st harmonic heating, which is the standard ICRF heating scheme used at JET; and H (He^3) and D (He^3) with low He^3 concentrations, 1%-2%, 1st harmonic heating. Schemes used to provide direct electron heating, include: H (He^3) 2nd harmonic; and D (He^3) and H (He^3) 1st harmonic with minority concentrations higher than 2%, to produce, respectively, standard and inverted mode conversion. Although, there is evidence for heating produced by mode conversion, unlike Alcator C-mod where mode-conversion has produced large co-current rotation [10], in JET there is no clear evidence of rotation caused by mode conversion. There is no significant difference in the rotation levels observed in either electron or ion heating schemes. The main difference is in the direction of rotation, since in the cases of direct electron heating the core counter rotated, while with dominant ion heating, in in particular the case of D plasmas with H minority both co- and counter-current rotation was observed (as illustrated in fig.1).

It is important to note the effect that the ICRF heating scheme and the antenna phasing can have on the rotation. With minority heating and an asymmetric phasing (i.e. either $+90^o$ phasing resulting in launched waves propagating predominantly in the co-current direction or -90^o phasing resulting in launched waves propagating predominantly on the counter-current direction), a small toroidal momentum in either co– or counter-current can be produced. Experimentally it has been found that antenna phasing has small effects on the core rotation (~3krad/s) [7]. In the case of minority heating it was also shown that the minority resonance layer position could have an effect on the core rotation, as has the minority concentration level [7].

There isn't a significant difference between the angular frequencies observed at the edge in ICRF and Ohmic heated plasmas (fig.2) and in plasmas with LHCD [8], indicating that ICRF heating drives rotation mostly in the plasma core.

2.2 OHMIC HEATING

In most experiments with ICRF, rotation measurements during Ohmic phases, either before the ICRF heating or sometime after (at least 1 s after) the heating was switched off. Angular frequency profiles are hollow showing counter-current rotation in the core, with co-current rotation in the outer plasma (fig.2). No dedicated experiments to study the effect of density on rotation have been performed. Thus it is not known if core rotation from may change direction above a density threshold as observed in TCV [11] and Alcator C-mod [12].

2.3 LHCD

The LHCD system in JET is mainly used to control the q-profile in advanced plasma scenarios, where a negative magnetic shear in the core can lead to the formation of internal transport barriers. In order to study the effect of magnetic shear on intrinsic rotation, measurements had been previously made in plasmas with by LHCD added during the current ramp phase. These discharges with a slightly reversed q profiles and $q > 1$ showed peaked co-rotation [8]. More recently, rotation has been measured in plasmas with LHCD, with powers up to 4MW, added later in the discharges when a $q = 1$ surface is already present. In all cases with LHCD applied later the core was counter-rotating. A comparison of discharges with similar LHCD power, toroidal field and density (fig.3) indicates that the difference in core magnetic shear may have influenced the direction of rotation.

One should remark here that the effect that the LH waves deposition profile may have on rotation has not yet been accessed, as no dedicated experiments have been performed to find out how rotation could depend on toroidal field and density that are parameters affecting LH wave penetration. In addition, it should be noted that the application of LH power can in itself affect the rotation, since the LH waves carry wave momentum. This effect was assessed in reference [8] where it was found to be small, less than 1 krad/s in the centre.

3. SCALING OF ROTATION WITH NORMALISED BETA (JET STANDARD RIPPLE $\delta_{TF} = 0.08\%$)

Recently, we focused on observations in ICRF heated ELMy H-mode plasmas with high-normalised beta [1]. The JET data from ELMy H-modes not previously included in a multi-machine database were compared with a scaling for the Alfven-Mach number, and a scaling for the velocity change from L-mode into H-mode [5]. These two scalings, derived for co-rotating plasmas, do not reproduce well the JET data, where rotation can be lower for the same beta normalized.

At JET no significant difference between H-mode and L-mode rotation is observed, except that the H-mode velocities near the edge are generally slightly lower than in Lmodes.

In a few ELMy H-modes the edge was seen to counter-rotate (see fig.4).

In figures 5 and 6 JET H-mode data is added to plots taken reference [5].

4. SCALING FOR COUNTER-CURRENT ROTATION (JET STANDARD RIPPLE $\delta_{TF} = 0.08\%$))

In either L-mode or in H-mode, core counter-rotation is a common observation in JET plasmas. JET intrinsic rotation profiles in all heating scenarios are often observed to change sign from co-rotation in the edge to counter-rotation in the core. In view of models of turbulent momentum transport that predict that changes in rotation might be correlated to gradients of bulk plasma parameters, the possible correlation of JET core rotation with electron and ion temperatures and plasma density is being investigated.

A dependence of core rotation with plasma current, I_p, had been found previously for JET Lmodes with ICRF minority heating, core counter-rotation being observed mostly for low plasma currents ($I_p < 2$ MA) [8]. We can now confirm that central counter rotation in Ohmic plasmas is also inversely proportional to I_p. For JET Ohmic heated cases, the velocity in the counter-current direction generated in the core, ΔV_φ was found to be proportional to ΔT_i,/I_p, the ion temperature difference in the core divided by the plasma current. This linear scaling, with a proportionality constant of order 10km/s MA/keV is similar to a previous observation in TCV [13]. This is shown in figure 7, a plot of $I_p \Delta V_\varphi$ versus ΔT_i for hollow rotation profiles, where $\Delta V\varphi$ is the difference between maximum and minimum rotation frequency as indicated above in figure 1a, and ΔT_i is the difference between central and edge T_i. Data from TCABR [14] a much smaller tokamak have also been ploted, showing a scaling of counter-rotation with ΔT_i and I_p that is independent of machine size. For comparisonwe have also plotted in fig.7 data from hollow rotation profiles obtained in JET ICRF heated plasmas with minority heating and DIII-D [15] plasmas with ECRF heated. Although the data scattering is large, the auxiliary heated JET and DIII-D plasmas lye close to the scaling obtained for the Ohmic plasmas.

This experimental scaling can be derived from simple theoretical arguments based on the symmetry properties of the turbulent transport of toroidal angular momentum [4] as

$$I_p \, \Delta V_\varphi = \alpha \, c^2/e \, \Delta T_i \tag{1}$$

In fig.7, the line is the least-square fit of the data to expression (1). The slope is $\alpha = 18 \text{km}\cdot\text{s}^{-1}\cdot\text{MA}\cdot\text{keV}^{-1}$.

5: EXPERIMENTS WITH ENHANCED TOROIDAL FIELD RIPPLE

The JET rotation database includes pulses with different magnetic field ripple, δ_{TF} (where $\delta_{TF} = (B_{max}-B_{min})/(B_{max}+B_{min})$, with B_{max} and B_{min} being the maximum and minimum toroidal field values). The effect of the magnetic field ripple on intrinsic rotation was assessed with δ_{TF} values ranging from δ_{TF} ~0.08%, which is the JET standard low ripple configuration, to an enhanced δ_{TF} up to 1.5% [6]

In order to separate ripple fast-ion effects from thermal ion effects rotation was measured in Ohmic and in ICRF heated plasmas. In both cases ripple causes counter rotation, indicating a strong torque due to non-ambipolar transport of thermal ions and in the case of ICRF also fast ions.

Figures 8-10 illustrate ripple effects in plasmas with ICRF heating. Figure 8 shows how counter rotation increased with ripple in the edge and the core. In figures 9-10, a plasma co-rotating at 1% ripple, becomes entirely counter rotating at 1.5% ripple. The core counter-rotation increases further before a monster sawtooth crashes when core-tae modes are present and fast-ion losses observed.

CONCLUSIONS

Intrinsic plasma rotation has been measured in JET plasmas with Ohmic heating, ICRF heating and LHCD. Several ICRF schemes were used, some with dominant ion heating, others providing direct electron heating including experiments of mode conversion. Although most are L-mode plasmas, there are a few cases of H-modes obtained with ICRF heating.

There are no significant differences between levels of intrinsic rotation measured in L-modes and H-modes. Typical C6 toroidal velocities are less than 30km/s in all scenarios. The main difference is in the direction of rotation. The edge is normally co-rotating however there are a few examples of edge counter-rotation in ELMy H-modes with type I ELMs. With ICRF minority heating and with LHCD the plasma core were observed to rotate in either co- or counter-current direction.

The possible reasons for core counter-rotation were investigated experimentally. Some factors clearly influencing the direction of rotation in the core are details of the heating scheme, magnetic shear, plasma current and MHD activity. Counter rotation was found to increase in the presence of MHD activity via losses of fast ions. One should note that counter-rotation is observed in cases of direct electron heating with ICRF, Ohmic and most LHCD cases.

An important factor influencing core rotation that was reported here was the safety factor, qprofile. This was studied by comparing discharges with LHCD. Peaked co-rotation was seen for the case with $q > 1$ and slightly reversed shear, while hollow counter-rotation was obtained for monotonic q profile with $q_0 \leq 1$.

A dependence of core rotation with plasma current had been found previously for JET Lmodes with ICRF minority heating, core counter-rotation being observed mostly for low plasma currents ($I_p < 2$MA) [8]. We show here that counter rotation is also inverse proportional to I_p in JET Ohmic plasmas. The velocity in the counter-current direction generated in the core is proportional to the ion temperature difference in the core divided by the plasma current, with a proportionality const. $\sim 10\text{km.s}^{-1}.\text{MA.keV}^{-1}$.

Toroidal field (TF) ripple was found to have a significant effect on the intrinsic rotation of plasmas without momentum input. Counter rotation increases with ripple in both Ohmic and in ICRF heated plasmas. Results show that ripple is likely to affect rotation in ITER and, should be taken into account in extrapolation from present data. At 0.5% ripple, JET plasmas were hardly rotating, while with 1% to 1.5% ripple H-mode plasmas with the whole plasma column counter-rotating were obtained.

Intrinsic rotation in JET plasmas, independent of the direction of rotation, is generally lower than expected from scaling laws that predict that rotation increases with normalized beta. JET results suggest that ITER intrinsic rotation may be substantially less than what was previously predicted by the multi-machine rotation scaling of ref. [5].

ACKNOWLEDGEMENTS

The first author acknowledges the support of EURATOM within the framework of the European Fusion Development Agreement and Fundação para a Ciencia e Tecnologia (FCT), Portugal.

REFERENCES

[1]. M.F.F. Nave et al., Plasma Physics and Controlled Fusion **54**, 074006 (2012)
[2]. T.A.K. Hellsten et al., Plasma Physics and Controlled Fusion **54**, 074007 (2012)
[3]. Y. Lin et al., Plasma Physics and Controlled Fusion **54**, 074001 (2012)
[4]. F.I. Parra et al., Physical Review Letters **108**, 095001 (2012)
[5]. J.E.Rice et al, Nuclear Fusion **47**, 1618 (2007)
[6]. M.F.F. Nave et al., Physical Review Letters **105**, 105005 (2010)
[7]. J-M Noterdaeme et al., Nuclear Fusion **43** 274 (2003)
[8]. L-G Eriksson et al Plasma Physics and Controlled Fusion **51** 044008 (2009)
[9]. L-G Eriksson, E. Righi and K-D Zastrow, Plasma Physics and Controlled Fusion **39** 27 (1997)
[10]. Y. Lin et al Physics of Plasmas **16** 056102 (2009)
[11]. A. Bortolon et al, Physical Review Letters **97** 235003 (2006)
[12]. J.E. Rice et al, Nuclear Fusion **51** 083005 (2011)
[13]. A. Scarabosio et al., Plasma Physics and Controlled Fusion **48**, 663 (2006).
[14]. J.H.F. Severo et al., Nuclear Fusion **43**, 1047 (2003).
[15]. J.S. deGrassie et al., Physics of Plasmas **14**, 056115 (2007).

Heating type	**Core**	**Edge**
Ohmic	*Counter*	*L-mode: co*
ICRH (ion absorption) *D(H),* $\omega=1\omega_c$	*Either co or counter*	*L-mode: co* *H-mode: co or counter*
H(He^3*),* $\omega=1\omega_c$ *D(He*^{3}*),* $\omega=1\omega_c$	*Counter*	*L-mode: co*
ICRH (electron heating) *H(He*^{3}*),* $\omega=2\omega_c$ *H(He*^{3}*),* $\omega=1\omega_c$ *(inverted mode- conversion)* *D(He*^{3}*),*$\omega=1\omega_c$ *(standard mode- conversion)*	*Counter*	*L-mode: co*
LHCD	*Either co or counter*	*L-mode: co*

Table 1:

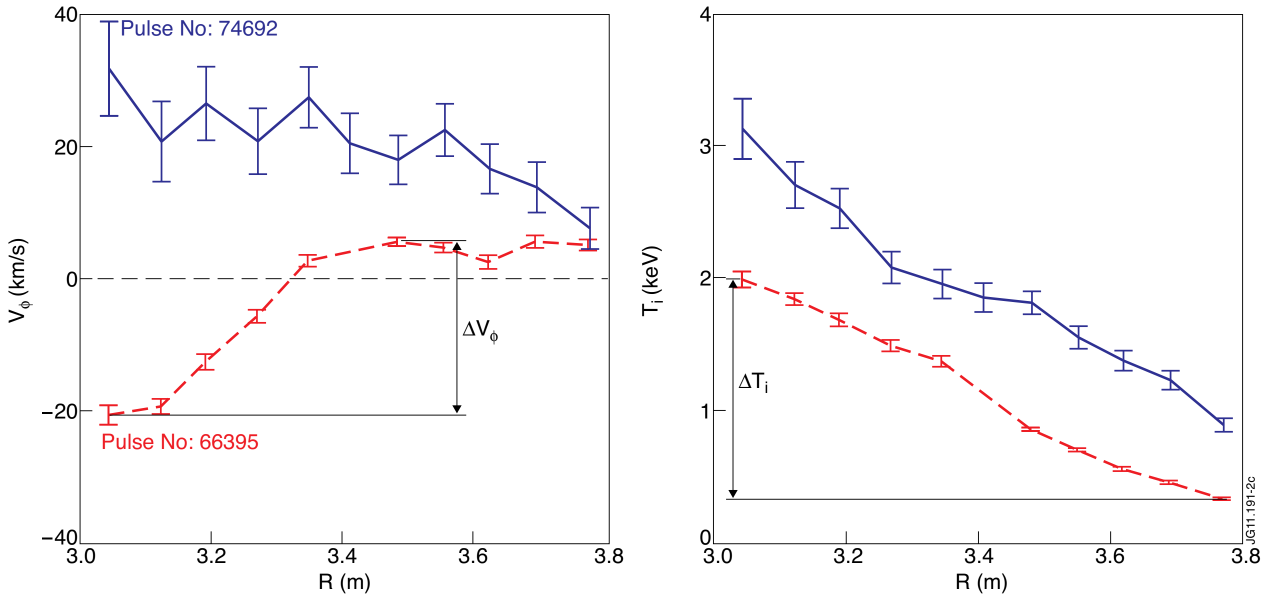

Figure 1: Illustration of C^6 intrinsic rotation profiles and ion temperature profiles in JET D plasmas with H minority ICRF heating, dipole configuration. Pulse 74692 with peaked rotation (P_{RF}=3.8MW, I_p = 2.06MA, B_T = 2.14T) and Pulse No: 66395 (P_{RF} =1.5MW, I_p = 1.45MA, B_T = 2.78) with hollow profile (Also indicated in the graphs are the definitions of $\Delta V\phi$ and ΔTi used later in fig.7.).

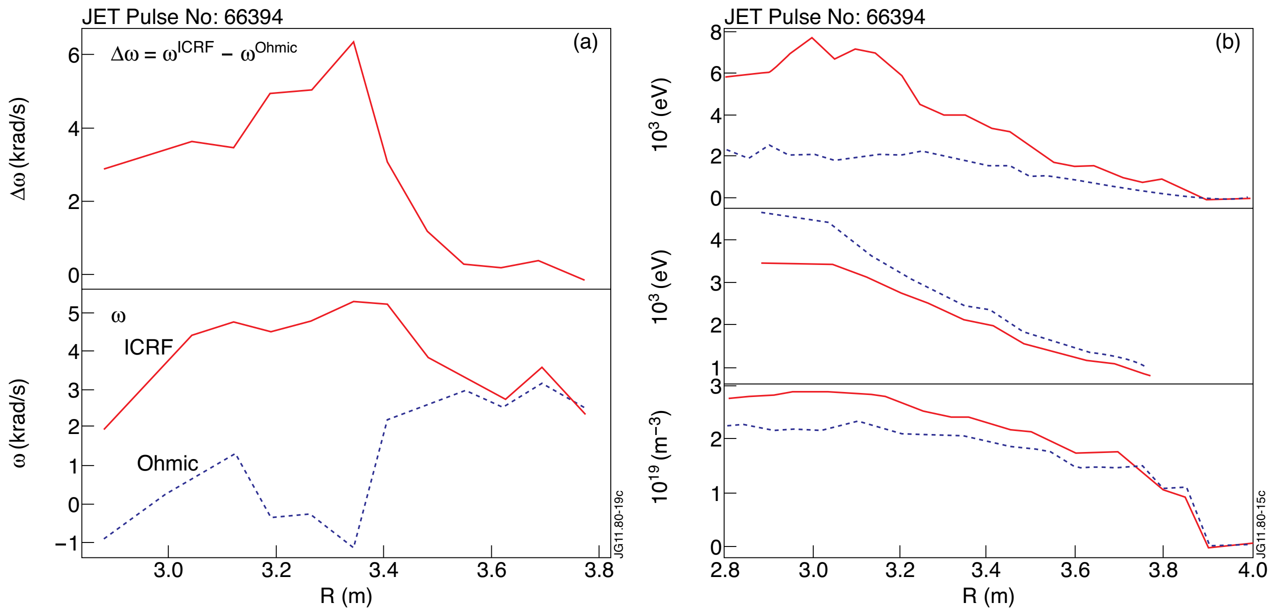

Figure 2: Rotation profiles for Pulse with P_{ICRF} = 4.8MW, H minority heating I_p = 2.4MA, B_T = 2.4T, f = 42MHz, n_H/n_D = 0.03, off axis heating on the high field side. a) The difference between the rotation profiles measured during Ohmic and ICRF phases, angular frequency profiles shown in the bottom; b) Electron temperature (top graph), ion temperature (middle graph) and density profile measured with LIDAR (bottom graph).

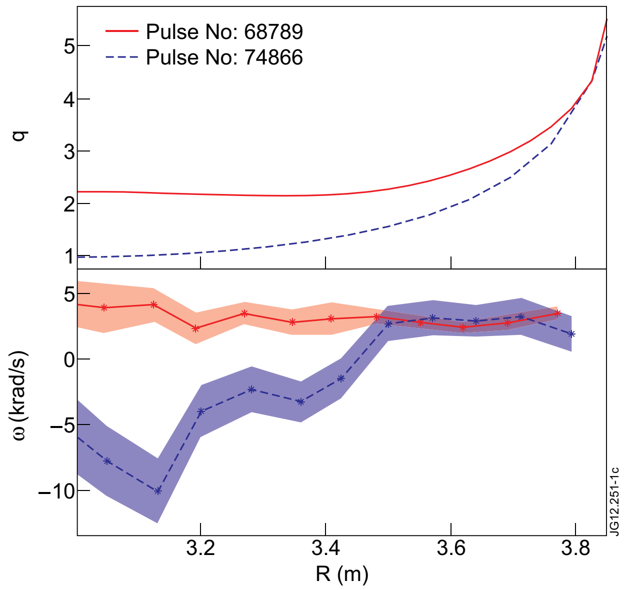

Figure 3: Plasmas with LHCD (Pulse No: 68789 with P_{LH} ~ 1.97MW applied during the I_{pramp}, I_p = 1.93MA, B_T = 2.78T, $<n_e>=1.98\times10^{19}$ m^{-3} and; Pulse 74866 with P_{LH} = 2.52MW applied later during I_p flat-top, I_p = 1.96MA, B_T = 2.44T, $<n_e>=2.09\times10^{19}$ m^{-3}). (top) Safety factor profiles and (bottom) C6 angular frequency profiles.

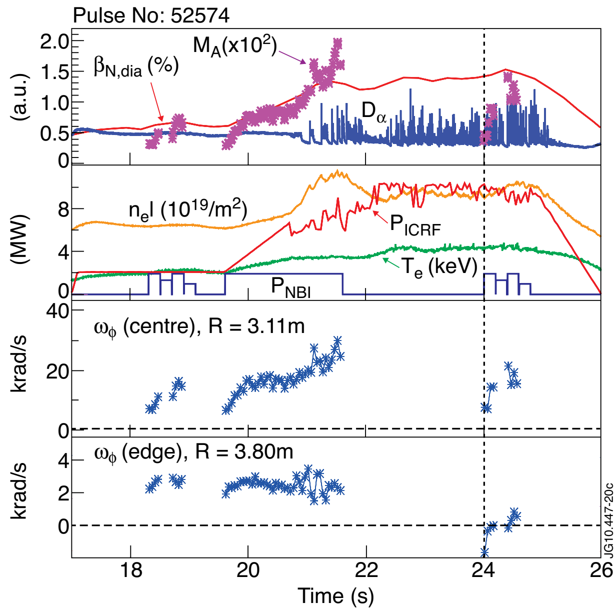

Figure 4: Pulse with P_{ICRF} ramped from 2 to 10MW, R_{res} = 2.7m, R_0 = 2.98m, I_p = 2MA, B_T = 2.45T, maximum β_N~1.3. The plots show: The vertical line indicates the time chosen for the data shown in figures 5-6.

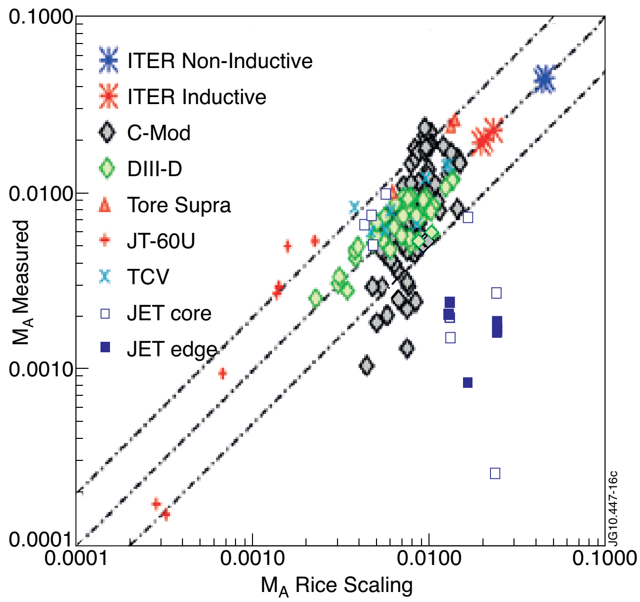

Figure 5: JET measured MA for H-mode plasmas added on figure 8 from Ref. [5]. Data from ELMy regimes is lower than predicted by the scaling derived in [5].

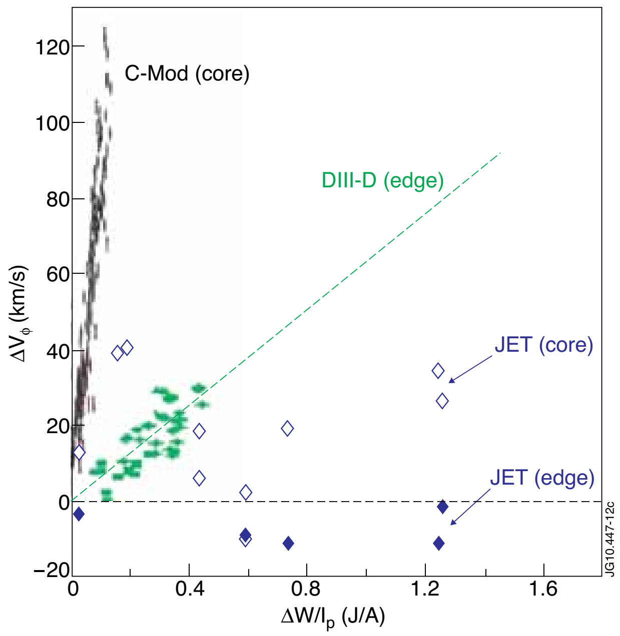

Figure 6: $\Delta V_\phi = V_\phi^{H\text{-}mode} - V_\phi^{L\text{-}mode}$ versus the change in plasma stored energy, W, divided by I_p, H-mode data from Alcator C-mod (r/a~0.1) and DIII-D (r/a~0.8) taken from figure 1 of ref. [5]. JET data in the plasma core (r/a'='0.1–0.39), and edge (r/a~0.8).

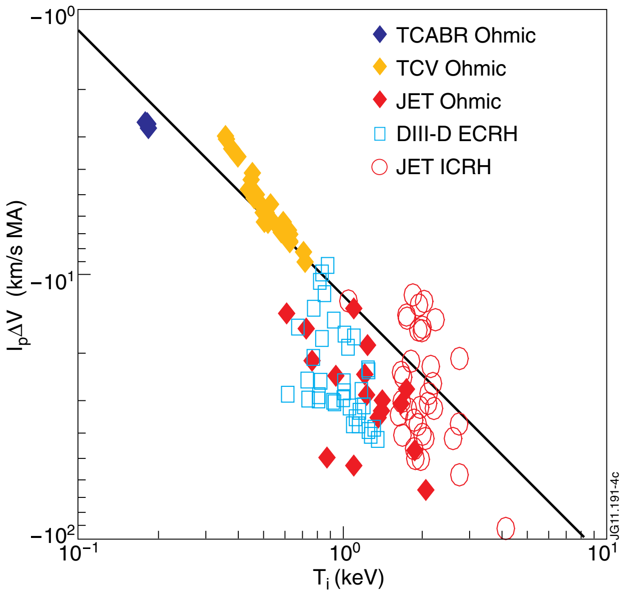

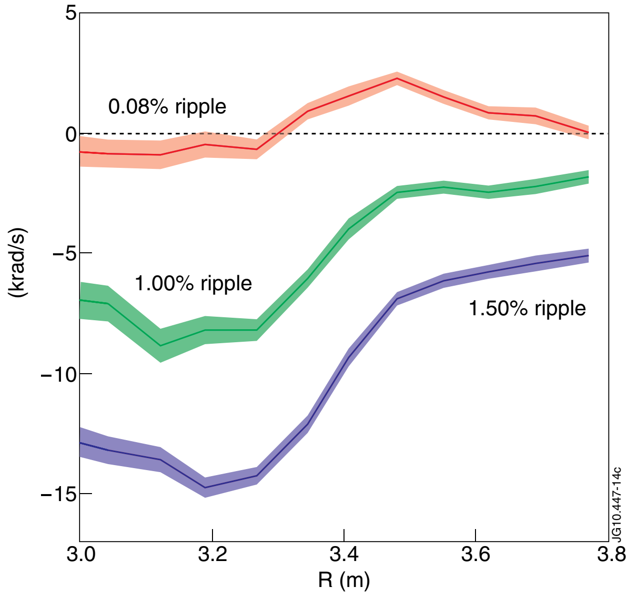

Figure 7: Toroidal velocity difference in the core ΔV_ϕ for hollow rotation profiles (see fig.1) multiplied by plasma current I_p against the ion temperature difference ΔT_i in the plasma core for machines with different sizes and different heating schemes: DIII-D, JET, TCABR and TCV.

Figure 8: C6 toroidal rotation angular frequency profiles during type III ELMy phases, at three ripple levels (with I_p = 1.5MA, <B_T>=2.2, P_{ICRF} ~3MW, H fundamental resonance slightly off-axis on the high-field side).

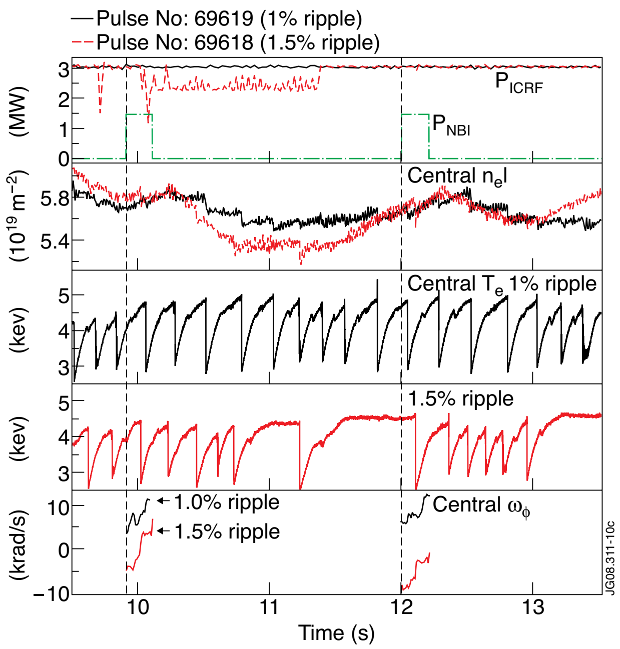

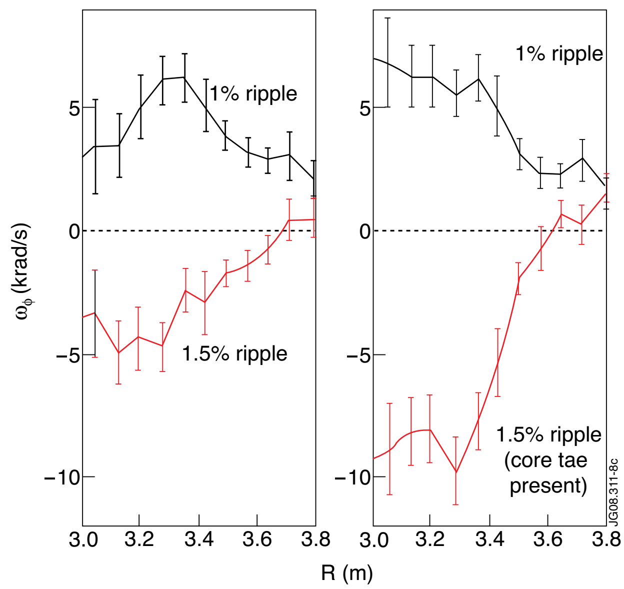

Figure 9: Discharges with P_{ICRF} = 4MW, I_p = 2MA, <B_T> = 2.1T with 1% and 1.5% ripple. The vertical lines indicate times of the angular frequency profiles shown in fig.10.

Figure 10: CX toroidal rotation profiles at the beginning of NBI blips (at t = 9.92s and at t = 12.01s). Counter-rotation is observed when ripple increases from 1% to 1.5%. Core counter rotation increases further before a monster sawtooth crash.